Received: 7 June 2021 | Accepted: 19 August 2021

DOI: 10.1111/gcb.15862

PRIMARY RESEARCH ARTICLE

Global Change Biology WILEY

Individual size distributions across North American streams vary with local temperature

Justin P. F. Pomeranz[1] | James R. Junker[2] | Jeff S. Wesner[1]

[1]Department of Biology, University of South Dakota, Vermillion, South Dakota, USA

[2]Great Lakes Research Center, Michigan Technological University, Houghton, Michigan, USA

Correspondence
Justin Pomeranz, Department of Biology, University of South Dakota, Vermillion, SD, USA.
Email: jfpomeranz@gmail.com

Funding information
National Science Foundation, Grant/Award Number: 1837233

Abstract

Parameters describing the negative relationship between abundance and body size within ecological communities provide a summary of many important biological processes. While it is considered to be one of the few consistent patterns in ecology, spatiotemporal variation of this relationship across continental scale temperature gradients is unknown. Using a database of stream communities collected across North America (18–68°N latitude, −4 to 25°C mean annual air temperature) over 3 years, we constructed 160 individual size distribution (ISD) relationships (i.e. abundance size spectra). The exponent parameter describing ISD's decreased (became steeper) with increasing mean annual temperature, with median slopes varying by ~0.2 units across the 29°C temperature gradient. In addition, total community biomass increased with increasing temperatures, contrary with theoretical predictions. Our study suggests conservation of ISD relationships in streams across broad natural environmental gradients. This supports the emerging use of size-spectra deviations as indicators of fundamental changes to the structure and function of ecological communities.

KEYWORDS
abundance size spectra, allometric scaling, biogeography, body size, bounded power law, community structure, freshwater ecology, individual size distributions, macroecology, macroinvertebrates

1 | INTRODUCTION

Detecting anthropogenic impacts on ecological communities remains an important goal for ecologists. Community based size-metrics, such as individual size distributions (ISD; also known as abundance size spectrum), have been proposed as a universal indicator of ecological status (Petchey & Belgrano, 2010). Many fundamental aspects of an organism's biology are controlled by body size, including metabolic rate, life history characteristics, diet breadth, and trophic position (Brown et al., 2004; Peters, 1983; West et al., 2001; White et al., 2007; Woodward et al., 2005). An individual's body size is tightly coupled with its metabolic rate (West et al., 2001) and body size also predicts biomass turnover at the population level (Brown et al., 2004). Due to gape limitation, particularly in aquatic environments, body size often determines predator–prey interactions, and is therefore related to trophic level (Barnes et al., 2010) and food web structure (Kerr & Dickie, 2001).

Communities are often characterized by a strong negative relationship between the abundance of individuals and body size (Sprules & Barth, 2015; White et al., 2007), and this decline is related to the trophic transfer efficiency between prey and their predators (Brown & Gillooly, 2003; Sprules & Barth, 2015; Trebilco et al., 2013). Therefore, size-based metrics offer an integrated measure for assessing ecological structure and function across communities (Perkins et al., 2018; Robinson et al., 2017), and can detect community-level responses to environmental stressors (Dossena et al., 2012; Jennings & Blanchard, 2004; Layer et al., 2011; Petchey & Belgrano, 2010; Pomeranz et al., 2019).

See Commentary on this article by Perkins, https://doi.org/10.1111/gcb.15862

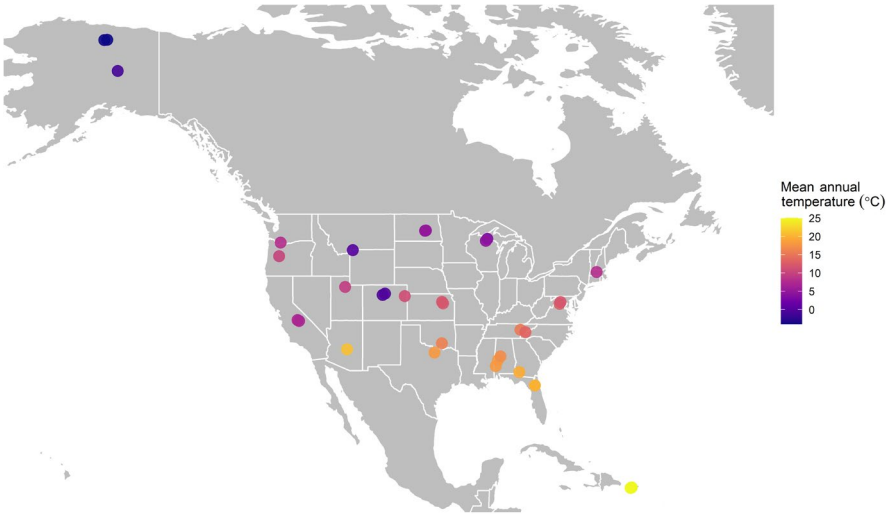

FIGURE 1 Map of site locations across North America. Points are color-coded based on mean annual temperature

Individual size distributions characterize the abundance (N) of individuals (regardless of species) with body size (M) and are well-described by a simple power law: $N \sim M^{\lambda}$. The exponent of this relationship is often estimated from the linear slope of log-log plots (i.e. $\log(N) = \lambda \times \log(M)$) after grouping individuals into bins based on body size. However, it can also be estimated directly using maximum likelihood methods (Robinson et al., 2017; Sprules & Barth, 2015; White et al., 2008). Throughout the rest of this paper, "size spectra slopes" refers to the slope of the relationship in log-log transformed variables, and "ISD exponent" refers to the maximum likelihood estimate of individual-level data (Supporting Information). The ISD relationship has theoretical backing based on metabolic scaling theory (Brown et al., 2004) and has received strong empirical support from a number of studies from diverse ecosystems (Blanchard et al., 2017; Jennings & Blanchard, 2004; Mazurkiewicz et al., 2019, 2020; Sheldon et al., 1972; Trebilco et al., 2013).

Because size spectra are based on body size and body size is influenced by temperature (Atkinson, 1994; Bergmann, 1847), it is widely expected that size spectra will change across gradients of environmental temperature. This prediction is derived from several ecological rules (e.g., temperature-size rule in individuals, Atkinson, 1994; smaller mean body size across populations, Bergmann, 1847) and forms a central tenet of macroecological theory (e.g., Baiser et al., 2019). In general, increases in temperature are predicted to lead to steeper (more negative) ISD exponents due to a relative decrease in large versus small individuals (Daufresne et al., 2009; Gardner et al., 2011; O'Gorman et al., 2017; Sheridan & Bickford, 2011). This prediction assumes that temperatures will disproportionately affect larger organisms, increasing the proportion of smaller species and the proportion of young age classes, and decreasing maximum body size or size-at-age (Daufresne et al., 2009). However, widespread empirical support for steeper size spectra at higher temperatures is ambiguous and includes notable deviations. For example, in Icelandic streams spanning a large natural temperature gradient, warmer streams had shallower size spectra slopes and supported a higher relative abundance of large body sizes than similar cold streams. Likewise, total community biomass was higher in warm streams (O'Gorman et al., 2017). Across ocean reefs, warmer temperatures were associated with both shallower ISD relationships and higher community biomass (Robinson et al., 2017), suggesting that temperature may not only modify the distribution of biomass and individuals among body sizes, but also alter the total biomass ecosystems can support. The transfer of energy through food webs and the support of biomass are directly tied to crucial ecosystem services. In the face of continued climate warming, reconciling the conflicting responses between theoretical expectations and empirical patterns of temperature on the distribution of body size and biomass within communities is critical for assessing the status of ecological communities.

A major limiting factor in large-scale studies of size spectra is the logistical challenge of obtaining consistently collected, processed, and analyzed data across a large spatiotemporal scale. To overcome this limitation, we measured community size spectra and biomass across stream sites in a large, coordinated ecological observation project, the National Ecological Observatory Network (NEON). Our primary objective in this study was to test the hypothesis that abundance size spectra in North American streams respond to environmental temperature.

2 | MATERIALS AND METHODS

Quantitative samples of benthic macroinvertebrates from NEON wadeable-stream sites from 2017 to 2019 were downloaded to determine the abundance size-spectra relationships (NEON, 2020b). NEON is a National Science Foundation (USA) funded program which collects standardized samples from 81 sites (24 streams) across a variety of terrestrial and aquatic ecosystems in North America. Repeat collections include automated instrument recordings and observational field sampling throughout the year, and data are available as open source data products (https://data.neonscience.org/home).

The wadeable-stream sites range across a broad climatic gradient (Figure 1), spanning 18 to 68°N latitude (majority between 33 to

45°N), mean annual air temperatures of −4 to 25°C, and mean annual precipitation of 331 to 2530 mm (Table S1). The stream width and depth were 8.6 ± 6.7 and 0.8 ± 0.4 (mean ± *SD*) meters respectively. Stream sites are primarily located in undeveloped settings (i.e. preserves, national parks, biological research stations, long term ecological research sites), but some are subjected to light agricultural or livestock grazing land use (Table S1).

Sites were sampled 1–4 times each year across the local growing season. Most sites had at least 2 years with three samples, except for Como Creek which only had 1 year with three samples (2018), and two samples collected in both 2017 and 2019. Additionally, three sites only had data available from a single collection in a single year; Red Butte Creek in 2018, Walker Branch and West St. Louis Creek both in 2019. Details of sample collection and processing protocols are available at the NEON website. Briefly, macroinvertebrate samples were collected from a known area using the sampling method most suited to a site. For example, Surber or Hess samples were used in shallow riffle or run sections with firm substrate (i.e., gravel and cobble), modified kicknets were used in deeper riffle or run sections, and a hand corer was used in sections with finer substrate such as sand or silt. All samples were processed in the laboratory by sieving with 250 μm mesh and were standardized based on the area sampled (Parker, 2018). Laboratory processing included subsampling for taxonomic identification and size class measurement (nearest mm) and estimating the total count of size class per species per sample. Size classes across the entire data set ranged from 1 to 65 mm and were recorded in 1 mm intervals. Estimated total counts per size class were standardized to individuals per m^2 by dividing by the area sampled (Chesney, 2019). Macroinvertebrate size classes (mm) were converted to individual dry mass (*M*, in mg) using published length-weight regression coefficients (Table S2). Most (96%) taxa had taxon-specific length-weight regressions and these were used for model development and assessment. Approximately 8% of the observations were flagged by NEON as being damaged, affecting their length measurements, and were removed from the data set. Individual estimated dry weights ranged from 1.0×10^{-3} to 1.2×10^{4} mg. Estimated ISD relationships are sensitive to the under sampling of small body sizes. Perkins et al. (2018) sampled benthic macroinvertebrates using comparable methods and found that body sizes smaller than 0.0026 mg were under sampled. Therefore, we set the minimum body size to 0.0026 mg estimated dry weight before estimating ISD relationships to avoid the under sampling of small body sizes. The final data set included over 13 million individual body sizes that ranged 7 orders of magnitude and represented a range of trophic levels (primary consumers, omnivores, and predators) and functional feeding groups (shredders, grazers, scrapers, filters feeders, predators).

Abundance size spectra parameters have been estimated using a variety of methods, with binning methods being common in the published literature (Edwards et al., 2017; Sprules & Barth, 2015; White et al., 2008). However, recent comparative studies have shown that binning methods provide biased parameter estimates, and recommend using maximum likelihood methods when individual data are available (Edwards et al., 2017, 2020; Sprules & Barth, 2015; White et al., 2008). Individuals in the NEON data set were measured to the nearest millimeter, and placed within a size class bin (i.e., size class 10 can contain individuals from 9.5 to 10.4 mm). Because the length-weight equations are exponential, the difference between dry weights based on the lower or upper edge of the bin can be substantial. Furthermore, since the length-weight regressions are taxon-specific, these biases can be exacerbated for some taxa. All of these factors can result in biased ISD relationship estimates. To address this, we used the extended likelihood method (MLEbin) of Edwards et al. (2020). The MLEbin method explicitly accounts for the uncertainty of body sizes within a bin. For example, it allows all the body sizes with size bin 10 to vary from 9.5 to 10.4 mm, instead of assuming that they are all equal to the mid-point of the bin, 10 in this example. For a detailed discussion of this method and a comparison to other commonly used methods for estimating ISD relationships, see Edwards et al. (2020).

To assess how the choice of method affected our results, we estimated exponent coefficients using six alternative methods including log-log regressions with different bin widths (Supporting Information S3). While the individual exponent estimates differed as expected among methods, the relationship between exponents and temperature was nearly identical among methods (Figure S2). Thus, our results are robust to alternative methods of calculating size spectra, and only the results of the MLEbin method (Edwards et al., 2020) are presented here. ISD plots for all collections at all sites, including the fit to a bounded power law, are available in Supporting Information S4. Note that the model estimates appear to be overfit at the smallest and largest body sizes, indicating that there may be some error associated with the specific value of ISDs reported here. However, as previously mentioned, our results are qualitatively similar regardless of the method employed.

We fit body size data (dry weight estimated from length-weight regressions) of macroinvertebrates from each collection to a bounded power law distribution with a probability density function:

$$f(x) = \frac{(\lambda+1)x^{\lambda}}{x_{\max}^{\lambda+1} - x_{\min}^{\lambda+1}} \quad \lambda \neq 1,$$

$$f(x) = \frac{1}{\log x_{\max} - \log x_{\min}} \quad \lambda = 1,$$

where x is body mass, λ is the scaling exponent of the ISD, and the distribution is bounded by the minimum (x_{min}) and maximum (x_{max}) body sizes observed in a collection. Maximum likelihood methods were used to estimate the ISD exponent, λ, using code modified from the *sizeSpectra* package in R (Edwards et al., 2017, 2020). Using these methods, a more negative ISD exponent represents a steeper decline in the abundance of larger body sizes (i.e. size spectra with a steeper slope in log-log space). Steep declines in the relative abundance of large individuals can be due to either a relative increase in the abundance of small body sizes, or a relative decrease in the abundance of large body sizes, or a

combination of the two. Regardless, steep ISD relationships represent a relatively smaller proportion of large individuals within a community.

In addition to the size spectra slopes, we also examined how total community biomass varied across the collections. First, we multiplied the biomass of individuals by their density to calculate grams of dry mass per m^2 for each sample within a collection ($n = 8$ samples per collection). Second, we averaged the sample estimates to get an estimate of the total community biomass within a collection.

Finally, to place our results into context, we compared the magnitude of change in ISD exponent across the temperature gradient (i.e. absolute difference between exponents at the highest and lowest temperature) to magnitudes reported for other studies. The other studies measured change in size spectra in response to temperature, but also in response to land use, commercial fishing, and acid mine drainage.

2.1 | Predictor variables

We were primarily interested in the relationship between mean annual temperature and size spectra. Both stream water and air temperature records are available across the sites, however, stream water temperature records are inconsistent in the lengths of total record and the annual period of observations (e.g., entire year vs. ice-free periods only). Generally, stream water temperature is tightly related to air temperature (Mohseni & Stefan, 1999; Pilgrim et al., 1998; Figure S1), therefore, we used the mean annual air temperature to maintain more consistent records across sites. Mean annual air temperature for each site was recorded from the site information available on the NEON website. Additionally, other environmental variables, specifically, nutrient availability, and resource subsidies (O'Gorman et al., 2017; Perkins et al., 2018) have been shown to affect size-abundance relationships. In order to control for the effects of these variables, we included them in a suite of candidate models and used model averaging to estimate the overall effect of mean annual air temperature (see Section 2.2 below). Total dissolved nitrogen and phosphorous observations for the NEON wadeable stream sites were downloaded and averaged across the sampling record at each site to characterize broad differences in nutrient availability among streams (n = 15–26 per annum, NEON, 2020a). Both nutrients were included because freshwater environments can be limited by either (Elser et al., 2007). As a proxy for external subsidies, average percent canopy cover was calculated for each site. Canopy cover is associated with increased terrestrial invertebrate and leaf litter input (England & Rosemond, 2004; Nakano et al., 1999). Percent canopy cover was obtained with replicate readings in the center and 0.3 m from the left and right banks of each stream (Scott, 2017) using a convex densiometer following methods of Ode et al. (2016). Finally, we included mean annual precipitation as a predictor variable in order to incorporate overall climate effects (Dodds et al., 2015). We acknowledge that there are potentially many other variables that could affect the relationship between ISD exponent and biomass in natural communities, and the limitations inherent in a natural survey study such as presented here. However, there are trade-offs between experimental control and spatiotemporal-scale, and our overall goal was to characterize how patterns of community size structure vary with temperature at the continental scale.

2.2 | Statistical analyses

To test the relationship between ISD exponents or standing stock community biomass and air temperature, we fit separate Bayesian hierarchical models with varying intercepts across sites and year. We chose a Bayesian approach because it easily incorporates prior information and hierarchical model structures (Dietze, 2017; Hobbs & Hooten, 2015; McElreath, 2020). For each model, ISD exponents or standing stock community biomass was the response. We fit eight candidate models for each response variable (16 models total). The models were as follows: (1) temperature only, (2) temperature + mean annual precipitation, (3) temperature + per cent canopy cover, (4) temperature + total dissolved nitrogen + total dissolved phosphorous, (5) temperature + per cent canopy cover + total dissolved nitrogen + total dissolved phosphorous (6) temperature + mean annual precipitation + per cent canopy cover + total dissolved nitrogen + total dissolved phosphorous, (7) temperature × total dissolved nitrogen, (8) temperature × total dissolved phosphorous. Models 1–6 were additive. Models 7 and 8 examined the interactive effects of nitrogen and phosphorous, with mean annual air temperature respectively. These interactions were included specifically because previous results have indicated that the relationship between size-abundance relationships and temperature may be inverted in the presence of high nutrient concentrations (O'Gorman et al., 2017). None of the predictor variables were strongly correlated (absolute value of all Pearson's correlation coefficients <.5 Figure S3). Predictor variables were standardized prior to analysis by subtracting the mean from each observation and dividing by the standard deviation (i.e. z-scores).

Because the ISD exponent (response variable) is continuous and can be positive or negative, we used a Gaussian likelihood. Priors for the intercept were *Normal*(−1.5,1). This puts low prior probabilities on positive exponents and on exponents with extreme negative values (e.g., <−4), reflecting a wide range of possible values reported in the size spectra literature (Blanchard et al., 2009; Edwards et al., 2017; White et al., 2007). Priors for the slope were *Normal*(0,0.25). Because 95% of the probability mass in a normal distribution lies within two standard deviations of the mean, this reflects the prior expectation that each standard deviation in a predictor variable could explain a change in the ISD exponent of ±0.5 units, which covers the range of observed variation in empirical studies of streams (i.e. change in coefficient of: −.15 O'Gorman et al., 2017; .13 Yvon-Durocher et al., 2011; −.19 McGarvey & Kirk, 2018). For both sigma and the standard deviation of the random site intercepts, a prior of *Exponential*(2) was set. The prior for the random year intercepts was set to *Exponential*(5) to improve model convergence. To ensure that the prior distributions contained reasonable prior predictions but did not overwhelm the posterior inference, we used prior predictive simulation and prior sensitivity analysis (see Supporting Information S4–S7; Gabry et al., 2019, Wesner & Pomeranz, 2021).

For community biomass, we used a Gamma likelihood with a log link, because biomass is a continuous and positive measure (Hobbs & Hooten, 2015). The model structure for biomass was the same as the model structure for the ISD exponent, λ. The prior for the intercept *Normal*(0,2). This reflects a prior expectation that average community biomass values up to ~50 g dry mass/m^2 are reasonable. These point estimates are obtained by exponentiating, due to the log-link, the prior mean (i.e. 0) plus and minus two standard deviations (exp(0−4) = 0.018, or exp(0 + 4) = 54.6). These values are compatible with the range of values reported in the literature (Benke et al., 1984; Grimm, 1988; Warmbold & Wesner, 2018). The remaining priors were *Normal*(0,1) for the slope coefficients (i.e. change of one standard deviation in predictor variable results in a change in biomass between ±2 orders of magnitude), *Exponential*(5) for the standard deviation of the random intercepts, and *Gamma*(0.01,0.01) for the shape parameter of the Gamma likelihood. As before, these priors were specified using prior predictive simulation and prior sensitivity analysis (Supporting Information S4–S7).

Models were specified using the *brms* package (Bürkner, 2018) in R (R Development Core Team, 2017), with posterior distributions derived using Hamiltonian Monte Carlo in *rstan* (Stan Development Team, 2018). The models were run using 4 chains each with 6000 iterations, in which the first half were discarded as warmup, resulting in 12,000 posterior draws. Convergence was checked by ensuring that all $\hat{r}$ were <1.1, and by visually assessing trace plots (Gelman & Rubin, 1992). To assess model fit, we used posterior predictive checks in which we simulated ten data sets from the posterior distribution and graphically compared them to the original data set (Gabry et al., 2019; Gelman et al., 2013; Figures S7 and S8). Strong visual discrepancies between the original data and simulated data indicate poor model fit (Gabry et al., 2019). In our simulations, both models produced data that were qualitatively similar to the original data, indicating good model fit. The overall effect of mean annual air temperature was estimated by averaging parameter estimates from candidate models by calculating model weights based on predictive posterior distributions using the Bayesian stacking method (Yao et al., 2018).

Prior and posterior distributions for parameter coefficients are plotted in Figures S5 and S6. A sensitivity analysis of our priors indicated our parameter coefficient estimates were robust to halving and doubling the *SD* value (Figure S9). The full hierarchical model structure can be found in Supporting Information S3.

3 | RESULTS

3.1 | ISD exponent

Maximum likelihood estimates of the ISD exponent, λ, ranged from −1.6 to −0.7 across individual collections. The median ISD of the model-averaged posterior distribution was −1.32 (95% CrI [−1.37, −1.26]; Table 1). The model-averaged coefficient estimate for the effect of mean annual air temperature on ISD exponent was −0.03 (95% CrI [−0.06, 0.003]) indicating a 97% probability that ISD exponents declined with temperature (Table 1). Estimated ISD exponents declined from −1.20 to −1.39 across the 29°C mean annual air temperature gradient (Figures 2a and 3a). This represented a similar change compared to other temperature-driven changes reported in the literature (Figure 4). However, it was much smaller than size spectra shifts reported in response to human disturbances like commercial fishing or acid mine drainage (Figure 4).

TABLE 1 Model-averaged coefficient estimates and 95% credible intervals explaining variation in individual size distribution exponents and community biomass across National Ecological Observation Network streams. All coefficient estimates for other models are available in the Supporting Information

Response	Coefficient	Median	Q2.5	Q97.5
λ exponent	Intercept	−1.32	−1.37	−1.26
	Temp	−0.03	−0.06	0.003
Biomass	Intercept	0.24	−0.25	0.77
	Temp	0.32	−0.04	0.69

3.2 | Community biomass

Community biomass showed higher variation among sites (Figure 2b) with collection-specific means ranging from 0.042 to 38 g dry mass/m^2. The model averaged coefficient estimate for the effect of mean annual air temperature on community biomass was 0.32 (95% CrI [−0.04. 0.69], Table 1). After exponentiating, this indicated that mean community dry mass increased by a factor of 1.4 for each standard deviation increase in temperature (Figure 2b) with a 96% probability of a positive relationship between community biomass and temperature.

Median biomass estimates ranged from a low of 0.29 g/m^2 at site Oksrukuyik Creek (site code: OKSR, mean annual air temperature: −4°C) to a high of 3.15 g/m^2 at site Lewis Run in Virginia (site code: LEWI, mean annual air temperature: 12°C; Figure 3b). The bimodal posterior distribution at Lewis Run in Figure 3b is a result of including models with and without total dissolved nitrogen. This site had the highest nitrogen value by far (~4 *SD* higher than the global mean), and when this predictor variable was not included the value of the random site intercept was much higher than when nitrogen was included (random site intercept estimates for the ISD exponent were similar regardless of whether or not nitrogen was included). To test the robustness of our results, we fit both the ISD and community biomass models without this site. The model-averaged coefficient estimate for the effect of temperature was not affected by the inclusion of Lewis Run (Table S5). There was no relationship between mean body size and temperature across the NEON sites (Figure S11), suggesting that differences in mean community biomass were primarily driven by changes in abundance rather than mean body size.

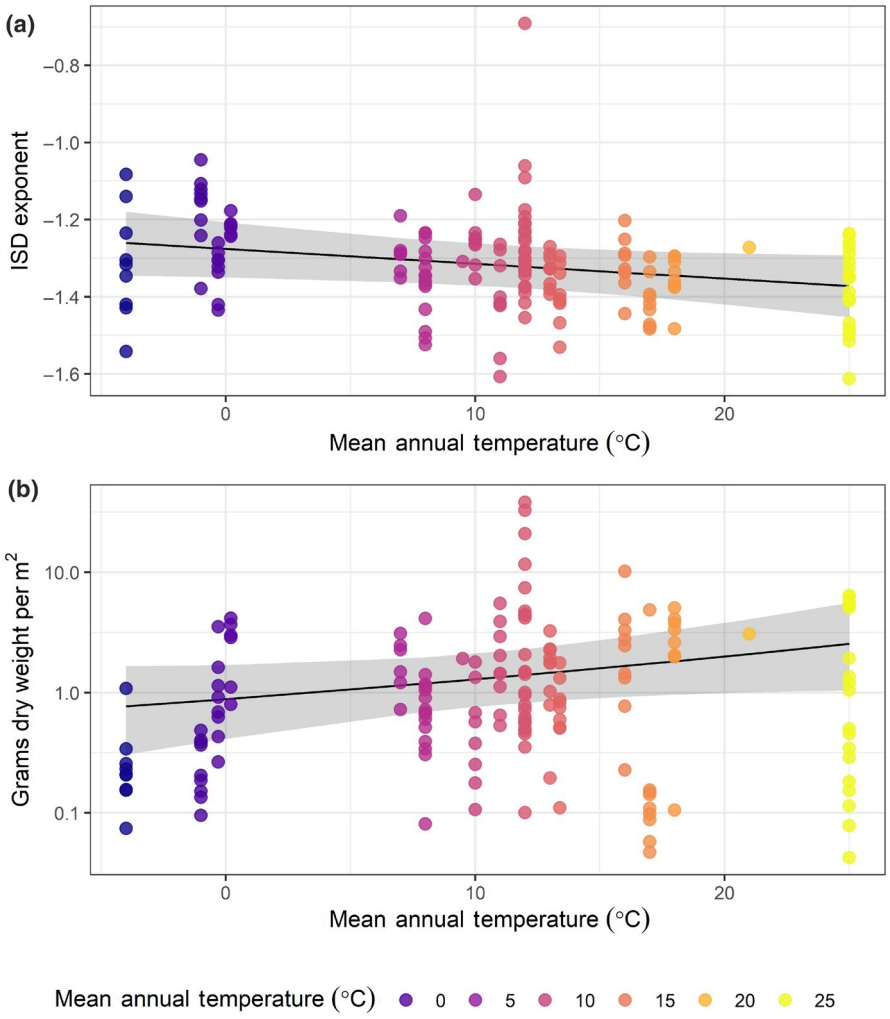

FIGURE 2 Relationship between mean annual temperature and (a) the ISD exponent of a bounded power law or (b) macroinvertebrate community dry mass at stream sites in the National Ecological Observation Network. Black lines and shading indicate the median and 95% credible intervals from the model-averaged estimate. Dots indicate individual exponent (a) or mean dry mass (b) observations for a collection and are color-coded by temperature. ISD, individual size distribution

4 | DISCUSSION

We analyzed a large collection of ISD relationships in stream communities and found that exponents became steeper with increasing air temperature across a broad temperature gradient. ISD exponents represent the efficiency of energy transfer from small, abundant, individuals to fewer large predators (Trebilco et al., 2013) with clear implications for ecosystem functioning (Cross et al., 2015; O'Gorman et al., 2012). Shallow exponents (less negative) indicate efficient transfer of energy (or higher availability of energy at the base of the food web) by supporting a relatively higher proportion of larger individuals, while steeper exponents (more negative) indicate inefficient energy transfer (or reduced energy availability at the base of the food web) with relatively fewer large individuals (Jennings & Mackinson, 2003; Trebilco et al., 2013). The more negative exponents reported here with increasing mean annual temperatures implies that warmer sites have a relatively lower proportion of large-sized individuals compared to colder sites. Indeed, there was a reduction in abundance of large sized individuals across the temperature gradient (Figure S13).

These results help to resolve previous uncertainty in how size spectra slopes scale with temperature. Variation in size spectra slopes is driven by variation in body size distributions and body size is in turn altered by temperature, either through reductions in taxon-specific body size, species turnover, or through changes in community structure (Atkinson, 1994; Bergmann, 1847; Daufresne et al., 2009; O'Gorman et al., 2012; Winder et al., 2009). Thus, it is widely expected that size-spectra slopes should vary across temperature gradients, though the direction of change is uncertain (Daufresne et al., 2009; Dossena et al., 2012; O'Gorman et al., 2012). O'Gorman et al. (2017) found that warmed Icelandic streams had shallower slopes, perhaps due to increased nutrient availability and changes in trophic transfer efficiency. In contrast, Dossena et al. (2012) found steepened slopes with temperature, but the effect varied over seasons. Likewise, seasonal variation in size spectra slopes was observed in West Virginia (USA) streams (although temperature was not tested directly, McGarvey & Kirk, 2018). These contrasting outcomes, derived from different experimental approaches, generate uncertainty in how ISD relationships should scale with temperature across large spatial gradients. By testing the size spectra-temperature relationship across a broad natural temperature gradient with repeated samples of size-spectra, the results here support the hypothesis that size spectra slopes become steeper at higher temperatures.

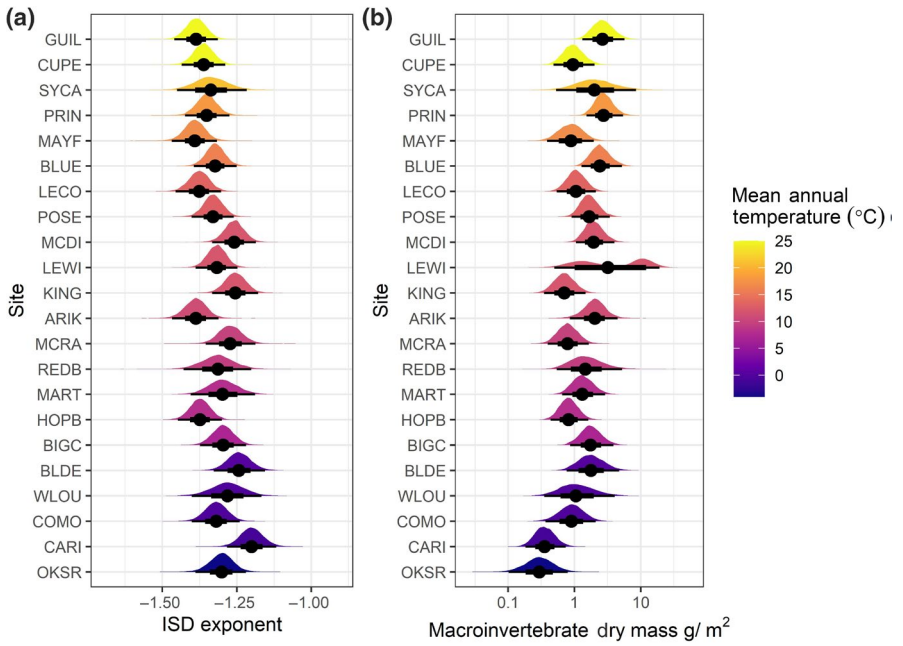

FIGURE 3 Posterior distributions of (a) ISD exponent and (b) mean dry mass across sites where color corresponds to mean annual temperature. Black point-intervals at bottom of density distributions show the median value and 66% (thick line) and 95% (thin line) credible intervals for a given collection. Sites are ordered by decreasing temperature from top to bottom (e.g., OKSR is the coldest site while GUIL is the warmest). ISD, individual size distribution

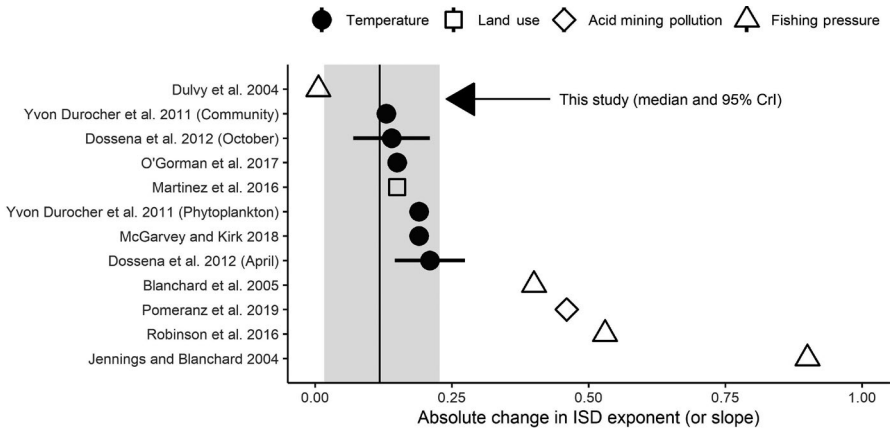

FIGURE 4 Range of effect sizes in the literature (shapes) compared to this study (mean and 95% CrI in vertical line and shading). Dossena et al. (2012) directly estimated the change in ISD exponent and reported a standard error. All other literature comparisons were made by subtracting the high and low estimates from group means. No estimate of uncertainty was possible from those studies. Studies used a mix of approaches to estimate size spectra exponents (or slopes), so these comparisons are approximate. ISD, individual size distribution

ISD exponents became steeper at higher temperatures, with median ISD exponents varying by ~0.2 units between the highest and lowest temperature. Direct comparisons of this effect size with previous studies of size spectra responses to temperature are hampered by the different approaches to estimating size spectra exponents (Edwards et al., 2017, 2020; White et al., 2008). However, the magnitude of our results are qualitatively similar to those presented in previous studies. For example, O'Gorman et al. (2017) reported that size spectra slopes calculated with log-log regression varied by ~0.15 units across a 20°C natural temperature gradient in streams. In freshwater mesocosms, size spectra slopes became steeper by up to 0.22 units in response to a 4°C increase in temperature (Dossena et al., 2012).

By comparison, the range of shifts reported in studies of temperature are dwarfed by those reported in response to more direct human-alterations of communities, like commercial fishing and acid mine drainage (Jennings & Blanchard, 2004; Pomeranz et al., 2019). Those studies report shifts that are ~3–6 times higher than those reported for temperature (Figure 4).

The variation in ISD exponents we observed is consistent with the expectation that size spectra represent a stable pattern of community structure (Jonsson et al., 2005; O'Gorman & Emmerson, 2011). One implication of this stability is that strong deviations in the ISD exponent may signify fundamental changes to the structure and function of ecological communities, which could be used to monitor ecosystem health (Petchey & Belgrano, 2010; Pomeranz et al., 2019). But it is not clear what represents a "strong" deviation. As shown from our literature comparison, changes in ISD exponents in response to external drivers vary by ~1.5 orders of magnitude, from ~0.03 to 0.75 units (Figure 4). However, in many cases, these shifts are from single

samples or isolated experiments. While these findings are important, longer term changes in size spectra are difficult to predict. By sampling repeatedly over several years and sites, our results overcome some of these limitations and offer several insights. First, individual samples of size spectra can vary widely around a central median (Figure 2a), indicating that multiple samples may be needed to avoid spurious conclusions. This is possibly driven by variation in local environmental conditions at the time of sampling, such as resource supply, flow conditions, and recent disturbances (or lack thereof) which are impossible to control in large-scale environmental survey studies. Second, across NEON streams at least, we would be surprised to see sustained shifts in size spectra that were larger than ~0.2 units (near the upper 95% CrI in Figure 4). Such a shift might indicate a relatively large underlying change in the community. Finally, the largest shifts in size spectra from the literature come not in response to temperature, but in response to commercial fishing and acid mine drainage (Figure 4). This emphasizes the need to understand how multiple stressors might interact to influence size spectra. For example, in marine fisheries, Blanchard et al. (2005) found that fishing was the primary driver of temporal change in size spectra, rather than temperature. Whether this is true in streams is unknown, but multiple stressors are common in freshwater ecosystems, indicating a clear opportunity to study their combined impacts on size spectra (Ormerod et al., 2010). Doing so is essential for understanding whether observed shifts in size spectra are within the range of natural variation or represent a fundamental change in community structure (Petchey & Belgrano, 2010).

In contrast with the negative relationship of size-spectra slopes with temperature, invertebrate community biomass increased across the temperature gradient. This was surprising given the strong theoretical support for lower biomass at higher temperatures (Brown et al., 2004; Saito et al., 2021). However, the predicted decline of standing biomass with temperature depends on a number of important conditions, first and foremost, that energy availability constrains abundance (Isaac et al., 2013) and second that there are consistent relationships between community body size and resource supply with temperature. Across the NEON streams there was no systematic relationship between mean body size and temperature (Figure S11). Quantifying resource supply is less straightforward as stream consumers utilize both autochthonous and allochthonous resources. Generally, rates of stream primary production increase with temperature (Demars et al., 2016) suggesting a positive relationship between temperature and resource supply which may confound expected temperature responses (e.g., Junker et al., 2020) and explain net positive relationships between invertebrate community productivity and temperature (e.g., Patrick et al., 2019). Whether these processes can explain the positive relationship between community biomass and temperature is unknown but is worth exploring.

Size-spectra relationships have been proposed as a universal indicator of ecological health, with deviations from "natural" size spectra representing disturbed systems (Jennings & Blanchard, 2004; Petchey & Belgrano, 2010; Trebilco et al., 2013). Yet defining "natural" is difficult without accounting for variation among broad spatial and temporal scales. By accounting for the effect of temperature on size spectra slopes in relatively undisturbed systems across 50° of latitude over 3 years, our results reveal bounds that could help to gauge the severity of size spectra change in response to disturbance. For example, one approach would be to compare size spectra from disturbed sites to the posterior predictive distribution of size-spectra at a similar site in our study, with deviations outside of the expected range of natural variation indicating the level of disturbance. This may represent a powerful tool for assessing ecological conditions. Indeed, as NEON data continues to be collected, it will be possible to compare our predictions to size-spectra collected after intense disturbances, such as extremely high or low flow events, temperature anomalies due to climate change, wildfires, flow debris, etc. This represents an exciting opportunity to test responses to disturbances at higher levels of organization, which has typically been difficult or impossible due to the large logistical efforts needed to collect community-wide data across broad spatial scales. Furthermore, data on post-disturbance size spectra within the NEON sites will provide valuable information on community recovery, and the magnitude, direction, and expected duration of altered ISD relationships.

ACKNOWLEDGMENTS

We thank CJ Perovich for thoughtful discussion and IA Sutton for help with maximum likelihood methods. This work was funded by an NSF EAGER award (DEB #1837233) to JSW and benefitted from comments on a previous version by D Perkins. During the writing of this manuscript, JSW was a Scientist in Residence at NEON.

CONFLICT OF INTEREST

The authors declare no conflicts of interest in the work presented here.

AUTHOR CONTRIBUTIONS

JP designed the study, collected the data, performed the analysis, made the figures, and wrote the first draft of the manuscript; JW performed the analysis, made the figures; JJ contributed to the figures; and all authors contributed substantially to revisions.

DATA AVAILABILITY STATEMENT

The data that support the findings of this study are openly available in the NEON data portal at https://www.neonscience.org/data, data product: DP1.20120.001, macroinvertebrate collection. R code to reproduce our results and figures is available at: https://github.com/Jpomz/Pomeranz-Junker-Wesner.

ORCID

Justin P. F. Pomeranz https://orcid.org/0000-0002-3882-7666
James R. Junker https://orcid.org/0000-0001-9713-2330
Jeff S. Wesner https://orcid.org/0000-0001-6058-7972

REFERENCES

Atkinson, D. (1994). Temperature and organism size—A biological law for ectotherms? *Advances in Ecological Research*, *25*, 1–58. https://doi.org/10.1016/S0065-2504(08)60212-3

Baiser, B., Gravel, D., Cirtwill, A. R., Dunne, J. A., Fahimipour, A. K., Gilarranz, L. J., Grochow, J. A., Li, D., Martinez, N. D., McGrew, A., Poisot, T., Romanuk, T. N., Stouffer, D. B., Trotta, L. B., Valdovinos, F. S., Williams, R. J., Wood, S. A., & Yeakel, J. D. (2019). Ecogeographical rules and the macroecology of food webs. *Global Ecology and Biogeography*, *28*(9), 1204–1218. https://doi.org/10.1111/geb.12925

Barnes, C., Maxwell, D., Reuman, D. C., & Jennings, S. (2010). Global patterns in predator–prey size relationships reveal size dependency of trophic transfer efficiency. *Ecology*, *91*(1), 222–232. https://doi.org/10.1890/08-2061.1

Benke, A. C., Arsdall, T. C. V., Gillespie, D. M., & Parrish, F. K. (1984). Invertebrate productivity in a subtropical Blackwater river: The importance of habitat and life history. *Ecological Monographs*, *54*(1), 25–63. https://doi.org/10.2307/1942455

Bergmann, C. (1847). Über die Verhältnisse der Wärmeökonomie der Thiere zu ihrer Größe. *Gottinger Studien*, *3*, 595–708.

Blanchard, J. L., Dulvy, N. K., Jennings, S., Ellis, J. R., Pinnegar, J. K., Tidd, A., & Kell, L. T. (2005). Do climate and fishing influence size-based indicators of Celtic Sea fish community structure? *ICES Journal of Marine Science*, *62*(3), 405–411. https://doi.org/10.1016/j.icesjms.2005.01.006

Blanchard, J. L., Heneghan, R. F., Everett, J. D., Trebilco, R., & Richardson, A. J. (2017). From bacteria to whales: Using functional size spectra to model marine ecosystems. *Trends in Ecology & Evolution*, *32*(3), 174–186. https://doi.org/10.1016/j.tree.2016.12.003

Blanchard, J. L., Jennings, S., Law, R., Castle, M. D., Mccloghrie, P., Rochet, M., & Benoît, E. (2009). How does abundance scale with body size in coupled size-structured food webs? *Journal of Animal Ecology*, *78*, 270–280. https://doi.org/10.1111/j.1365-2656.2008.01466.x

Brown, J. H., & Gillooly, J. F. (2003). Ecological food webs: High-quality data facilitate theoretical unification. *Proceedings of the National Academy of Sciences of the United States of America*, *100*(4), 1467–1468. https://doi.org/10.1073/pnas.0630310100

Brown, J. H., Gillooly, J. F., Allen, A. P., Savage, V. M., & West, G. B. (2004). Toward a metabolic theory of ecology. *Ecology*, *85*(7), 1771–1789. https://doi.org/10.1890/03-9000

Bürkner, P.-C. (2018). Advanced Bayesian multilevel modeling with the R package brms. *The R Journal*, *10*(1), 395–411. https://doi.org/10.32614/RJ-2018-017

Chesney, T. (2019). *NEON user guide to aquatic macroinvertebrate collection (NEON.DP1.20120)*. https://data.neonscience.org/data-products/DP1.20120.001

Cross, W. F., Hood, J. M., Benstead, J. P., Huryn, A. D., & Nelson, D. (2015). Interactions between temperature and nutrients across levels of ecological organization. *Global Change Biology*, *21*(3), 1025–1040. https://doi.org/10.1111/gcb.12809

Daufresne, M., Lengfellner, K., & Sommer, U. (2009). Global warming benefits the small in aquatic ecosystems. *Proceedings of the National Academy of Sciences of the United States of America*, *106*(31), 6. https://doi.org/10.1073/pnas.0902080106

Demars, B. O. L., Gíslason, G. M., Ólafsson, J. S., Manson, J. R., Friberg, N., Hood, J. M., Thompson, J. J. D., & Freitag, T. E. (2016). Impact of warming on CO_2 emissions from streams countered by aquatic photosynthesis. *Nature Geoscience*, *9*(10), 758–761. https://doi.org/10.1038/ngeo2807

Dietze, M. C. (2017). *Ecological forecasting*. Princeton University Press.

Dodds, W. K., Gido, K., Whiles, M. R., Daniels, M. D., & Grudzinski, B. P. (2015). The Stream Biome Gradient Concept: Factors controlling lotic systems across broad biogeographic scales. *Freshwater Science*, *34*(1), 1–19. https://doi.org/10.1086/679756

Dossena, M., Yvon-Durocher, G., Grey, J., Montoya, J. M., Perkins, D. M., Trimmer, M., & Woodward, G. (2012). Warming alters community size structure and ecosystem functioning. *Proceedings of the Royal Society B: Biological Sciences*, *279*(1740), 3011–3019. https://doi.org/10.1098/rspb.2012.0394

Edwards, A. M., Robinson, J., Blanchard, J., Baum, J., & Plank, M. (2020). Accounting for the bin structure of data removes bias when fitting size spectra. *Marine Ecology Progress Series*, *636*, 19–33. https://doi.org/10.3354/meps13230

Edwards, A. M., Robinson, J., Plank, M., Baum, J., & Blanchard, J. (2017). Testing and recommending methods for fitting size spectra to data. *Methods in Ecology and Evolution*, *8*(1), 57–67. https://doi.org/10.1111/2041-210X.12641

Elser, J. J., Bracken, M. E. S., Cleland, E. E., Gruner, D. S., Harpole, W. S., Hillebrand, H., Ngai, J. T., Seabloom, E. W., Shurin, J. B., & Smith, J. E. (2007). Global analysis of nitrogen and phosphorus limitation of primary producers in freshwater, marine and terrestrial ecosystems. *Ecology Letters*, *10*(12), 1135–1142. https://doi.org/10.1111/j.1461-0248.2007.01113.x

England, L. E., & Rosemond, A. D. (2004). Small reductions in forest cover weaken terrestrial-aquatic linkages in headwater streams. *Freshwater Biology*, *49*(6), 721–734. https://doi.org/10.1111/j.1365-2427.2004.01219.x

Gabry, J., Simpson, D., Vehtari, A., Betancourt, M., & Gelman, A. (2019). Visualization in Bayesian workflow. *Journal of the Royal Statistical Society: Series A (Statistics in Society)*, *182*(2), 389–402. https://doi.org/10.1111/rssa.12378

Gardner, J. L., Peters, A., Kearney, M. R., Joseph, L., & Heinsohn, R. (2011). Declining body size: A third universal response to warming? *Trends in Ecology & Evolution*, *26*(6), 285–291. https://doi.org/10.1016/j.tree.2011.03.005

Gelman, A., Carlin, J. B., Dunson, D. B., Vehtari, A., & Rubin, D. B. (2013). *Bayesian data analysis*. CRC Press http://www.stat.columbia.edu/~gelman/book/

Gelman, A., & Rubin, D. B. (1992). Inference from iterative simulation using multiple sequences. *Statistical Science*, *7*, 457–511. https://doi.org/10.1214/ss/1177011136

Grimm, N. B. (1988). Role of macroinvertebrates in nitrogen dynamics of a desert stream. *Ecology*, *69*(6), 1884–1893. https://doi.org/10.2307/1941165

Hobbs, N. T., & Hooten, M. B. (2015). *Bayesian models: A statistical primer for ecologists*. Princeton University Press.

Isaac, N. J. B., Storch, D., & Carbone, C. (2013). The paradox of energy equivalence. *Global Ecology and Biogeography*, *22*(1), 1–5. https://doi.org/10.1111/j.1466-8238.2012.00782.x

Jennings, S., & Blanchard, J. L. (2004). Fish abundance with no fishing: Predictions based on macroecological theory. *Journal of Animal Ecology*, *73*, 632–642. https://doi.org/10.1111/j.0021-8790.2004.00839.x

Jennings, S., & Mackinson, S. (2003). Abundance—Body mass relationships in size-structured food webs. *Ecology Letters*, *6*(11), 971–974. https://doi.org/10.1046/j.1461-0248.2003.00529.x

Jonsson, T., Cohen, J. E., & Carpenter, S. R. (2005). Food webs, body size, and species abundance in ecological community description. *Advances in Ecological Research*, *36*, 1–84. https://doi.org/10.1016/S0065-2504(05)36001-6

Junker, J. R., Cross, W. F., Benstead, J. P., Huryn, A. D., Hood, J. M., Nelson, D., Gíslason, G. M., & Ólafsson, J. S. (2020). Resource supply governs the apparent temperature dependence of animal production in stream ecosystems. *Ecology Letters*, *23*(12), 1809–1819. https://doi.org/10.1111/ele.13608

Kerr, S. R., & Dickie, L. M. (2001). *The biomass spectrum: A predator-prey theory of aquatic production*. Columbia University Press.

Layer, K., Hildrew, A. G., Jenkins, G. B., Riede, J. O., Stephen, J., Townsend, C. R., Woodward, G., Well-, L. D., Layer, K., Hildrew, A. G., & Jenkins, G. B. (2011). Long-term dynamics of a well-characterised food web: Four decades of acidification and recovery in the Broadstone Stream model system. *Advances in Ecological Research*, *44*, 69–117. https://doi.org/10.1016/B978-0-12-374794-5.00002-X

Mazurkiewicz, M., Górska, B., Renaud, P. E., Legeżyńska, J., Berge, J., & Włodarska-Kowalczuk, M. (2019). Seasonal constancy (summer vs. winter) of benthic size spectra in an Arctic fjord. *Polar Biology*, *42*(7), 1255–1270. https://doi.org/10.1007/s00300-019-02515-2

Mazurkiewicz, M., Górska, B., Renaud, P. E., & Włodarska-Kowalczuk, M. (2020). Latitudinal consistency of biomass size spectra—Benthic resilience despite environmental, taxonomic and functional trait variability. *Scientific Reports*, *10*(1), 4164. https://doi.org/10.1038/s41598-020-60889-4

McElreath, R. (2020). *Statistical rethinking: A Bayesian course with examples in R and Stan*. CRC Press. https://xcelab.net/rm/statistical-rethinking/

McGarvey, D. J., & Kirk, A. J. (2018). Seasonal comparison of community-level size-spectra in southern coalfield streams of West Virginia (USA). *Hydrobiologia*, *809*(1), 65–77. https://doi.org/10.1007/s10750-017-3448-0

Mohseni, O., & Stefan, H. G. (1999). Stream temperature/air temperature relationship: A physical interpretation. *Journal of Hydrology*, *218*(3), 128–141. https://doi.org/10.1016/S0022-1694(99)00034-7

Nakano, S., Miyasaka, H., & Kuhara, N. (1999). Terrestrial-aquatic linkages: Riparian arthropod inputs alter trophic cascades in a stream food web. *Ecology*, *80*(7), 2435–2441.

National Ecological Observatory Network. (2020a). *Data product DP1.20093.001, chemical properties of surface water*. http://data.neonscience.org.

National Ecological Observatory Network. (2020b). *Data product DP1.20120.001, macroinvertebrate collection*. http://data.neonscience.org

O'Gorman, E. J., & Emmerson, M. C. (2011). Body mass-abundance relationships are robust to cascading effects in marine food webs. *Oikos*, *120*(4), 520–528. https://doi.org/10.1111/j.1600-0706.2010.18867.x

O'Gorman, E. J., Pichler, D. E., Adams, G., Benstead, J. P., Cohen, H., Craig, N., Cross, W. F., Demars, B. O. L., Friberg, N., Gíslason, G. M., Gudmundsdóttir, R., Hawczak, A., Hood, J. M., Hudson, L. N., Johansson, L., Johansson, M. P., Junker, J. R., Laurila, A., Manson, J. R., … Woodward, G. (2012). Impacts of warming on the structure and functioning of aquatic communities. Individual- to ecosystem-level responses. *Advances in Ecological Research*, *47*, 81–176. https://doi.org/10.1016/B978-0-12-398315-2.00002-8

O'Gorman, E. J., Zhao, L., Pichler, D. E., Adams, G., Friberg, N., Rall, B. C., Seeney, A., Zhang, H., Reuman, D. C., & Woodward, G. (2017). Unexpected changes in community size structure in a natural warming experiment. *Nature Climate Change*, *7*(9), 659–663. https://doi.org/10.1038/nclimate3368

Ode, P., Fetscher, E., & Busse, L. (2016). *Standard Operating Procedures (SOP) for the collection of field data for bioassessments of California wadeable streams: Benthic macroinvertebrates, algae, and physical habitat*. http://www.waterboards.ca.gov/swamp

Ormerod, S. J., Dobson, M., Hildrew, A. G., & Townsend, C. R. (2010). Multiple stressors in freshwater ecosystems. *Freshwater Biology*, *55*(Suppl. 1), 1–4. https://doi.org/10.1111/j.1365-2427.2009.02395.x

Parker, S. M. (2018). *AOS protocol and procedure: Aquatic macroinvertebrate sampling*. National Ecological Observatory Network. https://data.neonscience.org/documents/10179/2093436/NEON.DOC.003046vD/e8640e29-0875-44c0-9978-cf49b25c9ea0

Patrick, C. J., McGarvey, D. J., Larson, J. H., Cross, W. F., Allen, D. C., Benke, A. C., Brey, T., Huryn, A. D., Jones, J., Murphy, C. A., Ruffing, C., Saffarinia, P., Whiles, M. R., Wallace, J. B., & Woodward, G. (2019). Precipitation and temperature drive continental-scale patterns in stream invertebrate production. *Science Advances*, *5*(4), eaav2348. https://doi.org/10.1126/sciadv.aav2348

Perkins, D. M., Durance, I., Edwards, F. K., Grey, J., Hildrew, A. G., Jackson, M., Jones, J. I., Lauridsen, R. B., Layer-Dobra, K., Thompson, M. S. A., & Woodward, G. (2018). Bending the rules: Exploitation of allochthonous resources by a top-predator modifies size-abundance scaling in stream food webs. *Ecology Letters*, *21*(12), 1771–1780. https://doi.org/10.1111/ele.13147

Petchey, O. L., & Belgrano, A. (2010). Body-size distributions and size-spectra: Universal indicators of ecological status? *Biology Letters*, *6*, 434–437. https://doi.org/10.1098/rsbl.2010.0240

Peters, R. H. (1983). *The ecological implications of body size*. Cambridge University Press. https://doi.org/10.1017/CBO9780511608551

Pilgrim, J. M., Fang, X., & Stefan, H. G. (1998). Stream temperature correlations with air temperature in Minnesota: Implications for climate warming. *Journal of the American Water Resources Association*, *34*(5), 1109–1121. https://doi.org/10.1111/j.1752-1688.1998.tb04158.x

Pomeranz, J. P. F., Warburton, H. J., & Harding, J. S. (2019). Anthropogenic mining alters macroinvertebrate size spectra in streams. *Freshwater Biology*, *64*(1), 81–92. https://doi.org/10.1111/fwb.13196

R Development Core Team. (2017). *R: A language and environment for statistical computing*. R Core Team.

Robinson, J. P. W., Williams, I. D., Edwards, A. M., McPherson, J., Yeager, L., Vigliola, L., Brainard, R. E., & Baum, J. K. (2017). Fishing degrades size structure of coral reef fish communities. *Global Change Biology*, *23*(3), 1009–1022. https://doi.org/10.1111/gcb.13482

Saito, V. S., Perkins, D. M., & Kratina, P. (2021). A metabolic perspective of stochastic community assembly. *Trends in Ecology & Evolution*, *36*(4), 280–283. https://doi.org/10.1016/j.tree.2021.01.003

Scott, C. (2017). *NEON user guide to riparian vegetation percent cover (NEON.DP1.20191)*. https://data.neonscience.org/data-products/DP1.20191

Sheldon, R. W., Prakash, A., & Sutcliffe, W. H. (1972). The size distribution of particles in the ocean. *Limnology and Oceanography*, *17*(3), 327–340. https://doi.org/10.4319/lo.1972.17.3.0327

Sheridan, J. A., & Bickford, D. (2011). Shrinking body size as an ecological response to climate change. *Nature Climate Change*, *1*(8), 401–406. https://doi.org/10.1038/nclimate1259

Sprules, W. G., & Barth, L. E. (2015). Surfing the biomass size spectrum: Some remarks on history, theory, and application. *Canadian Journal of Fisheries and Aquatic Sciences*, *73*, 477–495.

Stan Development Team. (2018). *RStan: The R interface to Stan (2.18.2)* [Computer software]. http://mc-stan.org/

Trebilco, R., Baum, J. K., Salomon, A. K., & Dulvy, N. K. (2013). Ecosystem ecology: Size-based constraints on the pyramids of life. *Trends in Ecology & Evolution*, *28*(7), 423–431. https://doi.org/10.1016/j.tree.2013.03.008

Warmbold, J. W., & Wesner, J. S. (2018). Predator foraging strategy mediates the effects of predators on local and emigrating prey. *Oikos*, *127*(4), 579–589. https://doi.org/10.1111/oik.04676

Wesner, J. S., & Pomeranz, J. P. F. (2021). Choosing priors in Bayesian ecological models by simulating from the prior predictive distribution. *Ecosphere*.

West, G. B., Brown, J. H., & Enquist, B. J. (2001). A general model for ontogenetic growth. *Nature*, *413*(6856), 628–631. https://doi.org/10.1038/35098076

White, E. P., Enquist, B. J., & Green, J. L. (2008). On estimating the exponent of power-law frequency distributions. *Ecology*, *89*(4), 905–912. https://doi.org/10.1890/07-1288.1

White, E. P., Ernest, S. K. M., Kerkhoff, A. J., & Enquist, B. J. (2007). Relationships between body size and abundance in ecology. *Trends in Ecology & Evolution*, *22*(6), 323–330. https://doi.org/10.1016/j.tree.2007.03.007

Winder, M., Reuter, J. E., & Schladow, S. G. (2009). Lake warming favours small-sized planktonic diatom species. *Proceedings of the Royal Society B: Biological Sciences*, *276*(1656), 427–435. https://doi.org/10.1098/rspb.2008.1200

Woodward, G., Ebenman, B., Emmerson, M., Montoya, J. M., Olesen, J. M., Valido, A., & Warren, P. H. (2005). Body size in ecological networks. *Trends in Ecology & Evolution*, *7*, 402–409. https://doi.org/10.1016/j.tree.2005.04.005

Yao, Y., Vehtari, A., Simpson, D., & Gelman, A. (2018). Using stacking to average Bayesian predictive distributions (with discussion). *Bayesian Analysis*, *13*(3), 917–1007. https://doi.org/10.1214/17-BA1091

Yvon-Durocher, G., Montoya, J. M., Trimmer, M., & Woodward, G. (2011). Warming alters the size spectrum and shifts the distribution of biomass in freshwater ecosystems. *Global Change Biology*, *17*(4), 1681–1694. https://doi.org/10.1111/j.1365-2486.2010.02321.x

SUPPORTING INFORMATION

Additional supporting information may be found in the online version of the article at the publisher's website.

How to cite this article: Pomeranz, J. P. F., Junker, J. R., & Wesner, J. S. (2022). Individual size distributions across North American streams vary with local temperature. *Global Change Biology*, 28, 848–858. https://doi.org/10.1111/gcb.15862